Contents lists available at ScienceDirect

Electrochemistry Communications

Fabrication of the catalytic electrodes for methanol oxidation on electrospinning-derived carbon fibrous mats

Miaoyu Li, Gaoyi Han [*], Binsheng Yang [*]

Institute of Molecular Science, Key Laboratory of Chemical Biology and Molecular Engineering of Education Ministry, Shanxi University, Taiyuan 030006, PR China

A B S T R A C T

The carbon fibrous mats with high conductivity (50 S cm^{-1}) formed by carbon nanofibers with an average diameter of $\sim$150 nm have been fabricated by thermally treating the electrospun polyacrylonitrile fibers. The platinum clusters are electrodeposited on the carbon nanofibrous mats (CFMs) by multi-cycle CV method. In contrast to the catalytic peak current of methanol oxidation on commercial catalyst (185 mA mg^{-1} Pt), the catalytic peak current on optimum Pt/CFM electrode reaches to $\sim$420 mA mg^{-1} Pt despite of the large size (50–200 nm) of the Pt clusters, revealing that the special structure of carbon fibrous mats is favorable to improve the performance of catalyst.

© 2008 Elsevier B.V. All rights reserved.

1. Introduction

Direct methanol fuel cells (DMFCs) are now attracting enormous interest for applications in low emission vehicles, portable electronic devices and distributed home power generators because of their environmentally benign and high efficient properties used as power supply [1,2]. Usually, platinum and its alloy are used as catalyst for the oxidation of methanol in view of its high catalytic activity. However, the high cost of catalyst is one of main obstructions for the commercialization of DMFCs. It is one of the major endeavors to increase the catalytic efficiency of platinum and decrease its amount simultaneously [3].

It has been proved that the catalytic activity of platinum particles depends not only on the shape, size and distribution of the catalysts but also the categories and properties of the supporting materials [4]. Therefore, various carbon materials such as mesocarbon microbeads, ordered mesocarbon microbeads, activated carbon fiber and carbon nanotubes [5–8] have been used as catalysts supports for DMFCs. In order to avoid the low Pt utilization brought by ink-process, efforts have focused on finding the optimum material configurations to minimize the Pt loading and satisfy the requirements of reactant access, proton access, and electronic continuity [3].

Recently, electrospinning technique has been recognized as an efficient method to manufacture nanoscale fibrous structures [9]. Up to the present, organic, inorganic and organic–inorganic hybrid nanofibrous mats have been fabricated because of their potential applications in sensors, tissue scaffold and anodic material [9–14]. Considering the remarkable porous structure, close contact between the nanofibers and the high surface area of the electrospun fibrous mats, the catalyst particles deposited on the CFMs can satisfy the requirements of reactant access, proton access and electronic continuity for DMFCs. In this paper, we describe the fabrication of the catalytic electrodes Pt/CFM, and evaluate their performance for electrocatalytic oxidation of methanol.

2. Experimental

2.1. Reagents

Polyacrylonitrile (PAN) and Nafion (5%) solution were obtained from Aldrich. Chloroplatinic acid was purchased from Beijing Chemical Company. The commercial Pt/C (40 wt%) was obtained from Johnson Matthey Corp. And all other chemicals employed in this study were of analytical grade.

2.2. Apparatus

Scanning electron microscopy (SEM) and transmission electron microscopy (TEM) micrographs were taken on JEOL-JSM-6700F scanning electron microanalyser and H-600-2 microscope, respectively. Raman spectra were recorded on RM 2000 microscopic confocal Raman spectrometer (514 nm). XRD patterns were recorded on Bruker D8 Advance X-ray diffractometer (Cu Kα

radiation). The content of platinum was determined by an IRIS Advantage inductively coupled plasma atomic emission spectroscopy (ICP-AES) system. Specific surface areas were measured on an ASAP 2020m accelerated surface area and porosimeter system. The electrical conductivity was measured through four-point probe method. Electrochemical measurements were carried out on a CHI 660B electrochemistry workstation at 25 °C. The CFMs loaded with Pt or Pt/C, a platinum plate and saturated calomel (SCE) electrode was used as working, counter and reference electrode, respectively. The electrolyte was 0.5 mol L^{-1} H$_2$SO$_4$ + 1.0 mol L^{-1} CH$_3$OH aqueous solution for electrodes evaluation. High-purity argon flow was used for deaeration of the solutions and maintained above the electrolyte solution during measurements.

2.3. Fabrication of CFMs and electrodes

PAN (360 mg) dissolved in dimethylformamide (DMF, 4.0 mL) was used as electrospinning solution. The electrospinning potential was 13.7 kV, and the resulted fibers were collected on a sheet of electrically grounded aluminum foil placed 12 cm below the nozzle. The mats were peeled from the aluminum foil and transferred into a muffle furnace for oxidative stabilization at ~280 °C for 3 h in air. Then the oxidative stabilized fibrous mats were heated at 600 °C for 30 min firstly and then the temperature increased to 1200 °C and was kept for 1 h, under a high-purity argon atmosphere. The resulted CFMs (~50 μm thickness) were cut into strips with the size of 10 mm × 2.0 mm and used as electrodes directly. The platinum particles were deposited on the carbon nanofibrous mats by using multi-cycle CV in 0.5 mol L^{-1} H$_2$SO$_4$ + 2.0 mmol L^{-1} H$_2$PtCl$_6$ aqueous solutions. The potential window and the scan rate of the potential was optimized as −0.3 to 0.4 V and 100 mV s^{-1}, respectively. The obtained catalytic electrodes were denoted as Pt/CFM. By comparison, the commercial Pt/C loaded on the CFMs labeled as Pt/C electrodes had also been fabricated by transferring 6.4 μl of the ultrasonic-treated mixture of Pt/C catalyst (5.0 mg), water (1.25 mL) and Nafion solution (0.25 mL) onto the CFMs, and then evaporating the solvent at 80 °C. The content of Pt in the electrodes was about 0.21 mg cm^{-2}. And the geometric surface area of the electrodes was guaranteed to be about 0.04 cm^{-2}.

3. Results and discussion

PAN dissolved in DMF can be easily spun into white nanofibrous mats by electrospinning. The color of the PAN mats changes from white to dark-brown during the pre-oxidation process, and the black CFMs are obtained in a relatively high yield (~40%) after carbonization process. The CFMs are formed by long fibers with smooth surface and relatively uniform diameter ranging from 130 to 170 nm (average 150 nm). There are a large number of gaps in the mats, which is beneficial to deposition of Pt and diffusion of reactant (Fig. 1A). The Raman spectrum (Fig. 1B) shows the G-band (E$_{2g2}$ graphite mode) at 1588 cm^{-1}, and the D-band (defect-induced mode) at 1342 cm^{-1} [14]. The value of D/G (the intensity ratio of D-band to G-band) can be used to denote the relative content of graphite in the carbonaceous materials, and the value of D/G is 1.16 for our CFMs. The electrical conductivities of the CFMs are measured and found to be ~50 S cm^{-1}. However, the specific surface area of the CFMs is only ~7 m^2 g^{-1}. In contrast with the literature reported previously [14], our CFMs exhibit higher electrical conductivity and more content of graphite, and the reason may contribute to the more compact structure and the thinner diameter (average 150 nm) than that of literature (average 250 nm).

From the results shown in Fig. 2A, we can find that the optimum response current of methanol oxidation reaches to 90.0 mA cm^{-2} based on the geometric surface area on the Pt/CFM catalytic electrode prepared by 50 cycles CVs. In this case, the Pt electrodeposited on the CFMs is determined to be about 0.21 mg cm^{-2}, so the peak current can also be denoted as 419 mA mg^{-1}Pt. Then the Pt/CFM electrode prepared by 50 cycles is chosen as electrode for following testing. In 0.5 mol L^{-1} H$_2$SO$_4$ + 1.0 mol L^{-1} CH$_3$OH solutions, the curve for CFMs electrode shows no significant redox activity (Fig. 2B–a). However, the anodic current density on Pt/CFM electrode in the positively going scan increases with the increase of scan potential, and the peak current density reaches to 90.0 mA cm^{-2} (419 mA mg^{-1} Pt) at 0.78 V, which is significantly higher than 39.0 mA cm^{-2} (185 mA mg^{-1} Pt) at 0.70 V on commercial Pt/C electrode. In the reverse scan there is an anodic peak observed on both Pt/CFM and commercial Pt/C electrode, which can be attributed to the removal of the incompletely oxidized carbonaceous species formed in the positively going scan. The I_f/I_b value (0.90) for the Pt/CFM electrode is higher than that for the commercial Pt/C electrode (0.80), indicating that more intermediate carbonaceous species are oxidized to carbon dioxide in the anodic scan on Pt/CFM electrode [15].

Fig. 2C shows the anodic peak current densities of methanol oxidation on Pt/CFM and Pt/C electrodes during a total of 600 cycles. For both the electrodes, the anodic peak current density in positively going scan increases at initial cycles until it attains the maximum value and afterwards displays a downward trend with
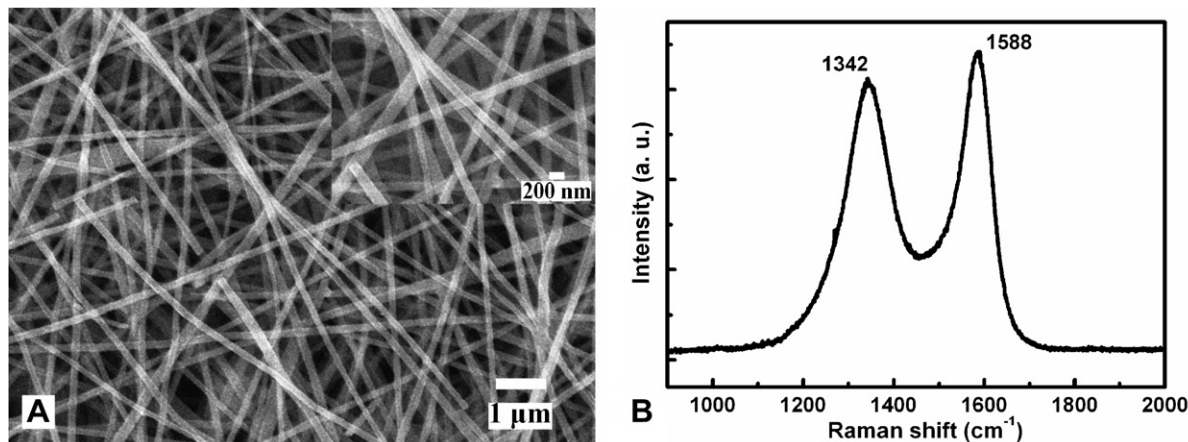

Fig. 1. (A) The SEM images and (B) the Raman spectrum of CFMs.
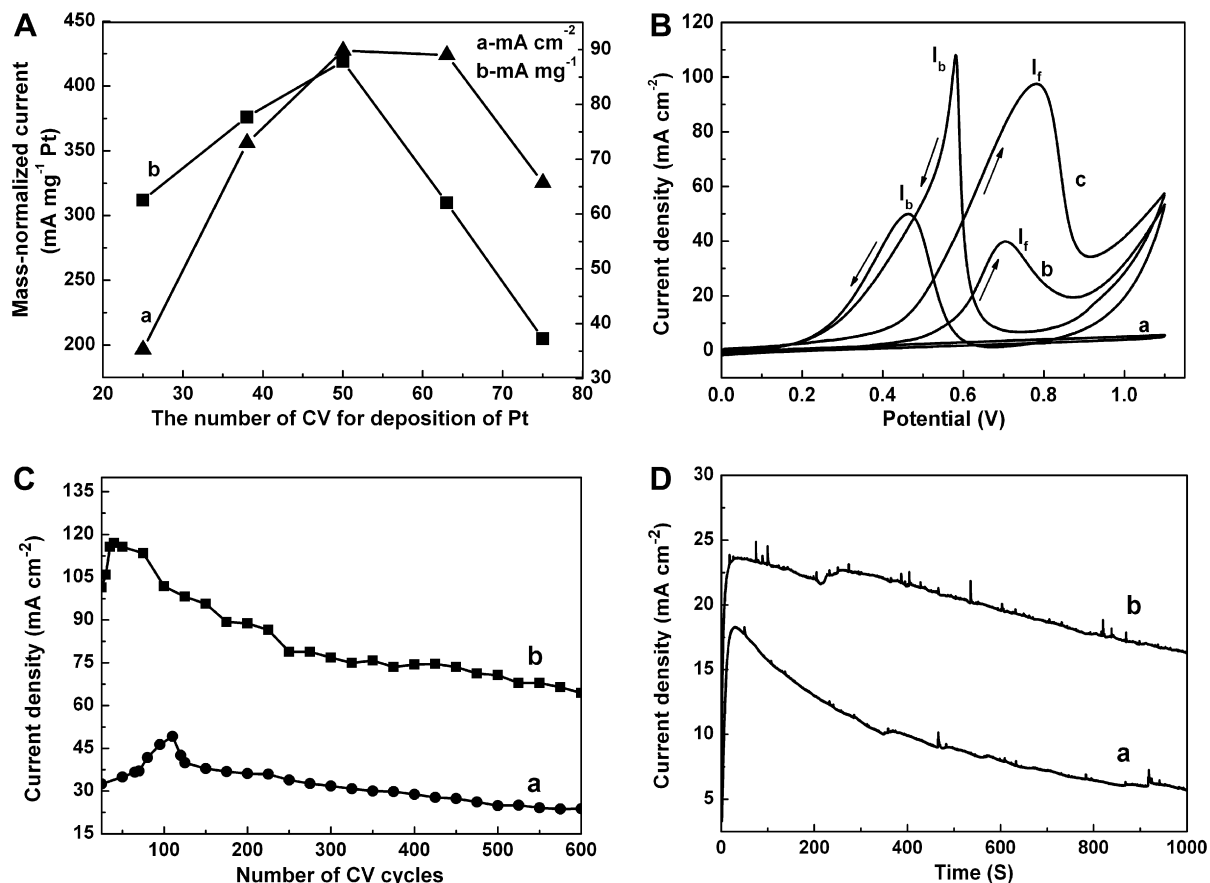
Fig. 2. (A) The plot of the peak current density of methanol oxidation on different Pt/CFM electrodes versus the cycle number of CV of Pt deposition, the potential scan rate is 100 mV s^{-1}, (B) cyclic voltammograms obtained for methanol oxidation on (a) CFM, (b) Pt/C and (c) Pt/CFM (Pt deposited by CV with 50 cycles) electrodes with the potential scan rate of 50 mV s^{-1}, (C) The plot of anodic peak current density of methanol oxidation on (a) Pt/C and (b) Pt/CFM electrode versus cycle numbers of CV with the potential scan rate of 100 mV s^{-1}, (D) Chronoamperometric curves of methanol oxidation on (a) Pt/C and (b) Pt/CFM at potential of 0.45 V.

the successive CV scans. For Pt/CFM electrode, the peak current density approaches a maximum of 117.5 mA cm^{-2} at the 40th cycle, and then decreases to 64.7 mA cm^{-2} at the 600th cycle, with a total decrease of 44.8%. However, the peak current density reaches its maximum (49.5 mA cm^{-2}) at the 109th cycle for Pt/C electrode, and then decreases to 23.9 mA cm^{-2} at the 600th cycle, with a total decrease of 51.4%.

Fig. 2D shows the curve of polarization currents density of methanol oxidation versus time at a constant potential 0.45 V. After the current densities reach their maximum, the current densities of methanol oxidation on both Pt/CFM and Pt/C electrodes present continuous decay with time increase. After a polarization time of 1000 s, there are 16.3 mA cm^{-2} and 5.7 mA cm^{-2} current densities remained on Pt/CFM and Pt/C electrodes, respectively. In addition, the decay of the current density on Pt/CFM electrode exhibits a more gently decreasing trend.

The SEM images show that the Pt clusters with irregular shapes and the size of 50–200 nm are dispersed on the surface of carbon fibers, and it is interesting to find that the fibers in inner layers of the mats are also coated by Pt clusters (Fig. 3A) in the Pt/CFM electrodes. Furthermore, we can find that the Pt clusters are formed by small Pt particles (5–10 nm, Fig. 3B, indicated by arrow) from the interface between the Pt and carbon surface (Fig. 3B). However, the Pt/C particles congregate together and cover the CFMs (Fig. 3C, inserted SEM image). Some particles are dispersed in the gaps between the carbon fibers (Fig. 3C), which leads to a loose contact between carbon fibers and catalyst particles. The

conductivity of Pt/C electrode is ~42 S cm^{-1}, which is 16% smaller than that of CFMs.

The broad diffraction peak at about 25.3° (Fig. 3D) is assigned to the diffraction of graphite crystallite (2 0 0), and the peaks at 39.9°, 46.3° and 67.7° are assigned to platinum (1 1 1), (2 0 0) and (2 2 0), respectively. According to the Scherrer formula ($d = 0.89\lambda/B\cos\theta$), the particle size of Pt is calculated on bases of Pt(1 1 1) peak, and the average diameter of Pt particles is found to be about 7.3 nm and 3.3 nm for Pt/CFM and commercial Pt/C, respectively. It should be noticeable that the Pt particles deposited on the carbon fibers surface congregate into cluster with a larger size (50–200 nm), which leads to a bad dispersivity of the Pt particles.

The performance of optimum Pt/CFM electrodes is superior to that of commercial Pt/C electrode in both the activity and stability although the dispersivity and size of Pt particles on CFMs are inferior to the commercial Pt/C catalyst. From the low specific surface area of the CFMs, the microstructure of the Pt/C electrode, and the conductivity decrease of the CFMs when commercial Pt/C loaded on CFMs, we may conclude that the high performance of the Pt/CFM electrode mainly comes from the relatively high conductivity of the carbon nanofibers mats and the close contact between Pt particles and carbon nanofibers, which makes the Pt catalyst exhibit high utilization efficiency [3]. It is expected that once the Pt particle size is reduced (e.g., 3.5 nm), or the dispersivity of Pt particles is increased through improving the synthesis method of Pt particles or improving the structure of the carbon nanofibers (such
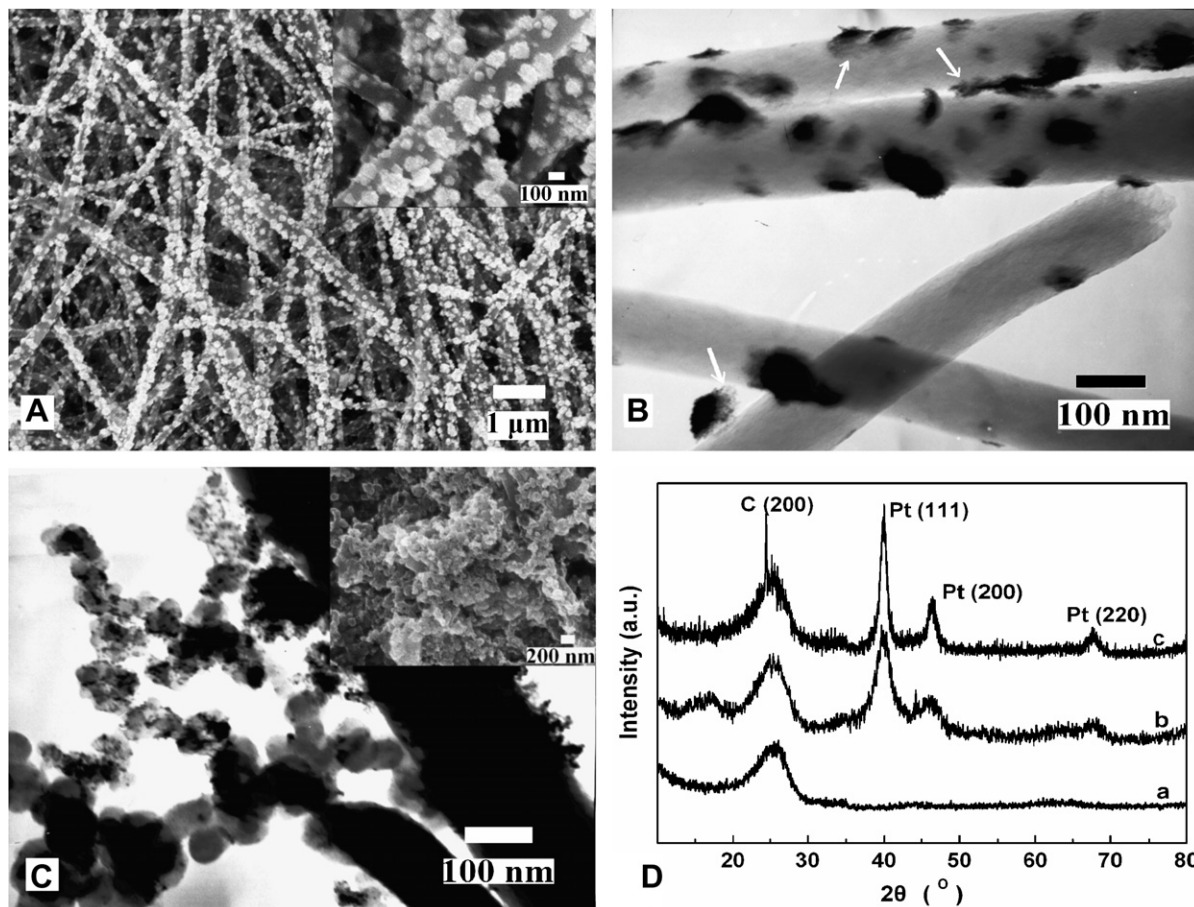
Fig. 3. The SEM images of (A) as prepared Pt/CFM electrode, (B) the TEM image of the same electrode as (A), (C) the TEM and SEM (inserted) images of as prepared Pt/C electrode and (D) the XRD patterns of the (a) as prepared CFMs, (b) commercial Pt/C (40 wt%) and (c) Pt/CFM.

as porous structure), the Pt/CFM electrodes will show superior performance.

4. Conclusions

The CFMs have been fabricated, and the platinum particles are deposited on the carbon fibers by multi-cycle CV method. The studies show that the platinum supported on CFMs exhibits high performance in the aspects of electrocatalytic activity and stability towards the oxidation of methanol. The carbon nanofibrous mats could be developed as new kind of supporting materials with higher performance for noble metal catalyst.

Acknowledgments

References

[1] H.S. Liu, C.J. Song, L. Zhang, J.J. Zhang, H.J. Wang, D.P. Wilkinson, J. Power Sources 155 (2006) 95.
[2] H. Uchida, Y. Mizuno, M. Watanabe, J. Electrochem. Soc. 149 (2002) A682.
[3] C. Wang, M. Waje, X. Wang, J.M. Tang, R.C. Haddon, Y.S. Yan, Nano Lett. 4 (2004) 345.
[4] G. Selvarani, A.K. Sahu, N.A. Choudhury, P. Sridhar, S. Pitchumani, A.K. Shukla, Electrochim. Acta 52 (2007) 4871.
[5] Y.C. Liu, X.P. Qiu, Y.Q. Huang, W.T. Zhu, J. Power Sources 111 (2002) 160.
[6] S.H. Joo, C. Pak, D.J. You, S.A. Lee, H.I. Lee, J.M. Kim, H. Chang, D. Seung, Electrochim. Acta 52 (2006) 1618.
[7] H.X. Huang, S.X. Chen, C.E. Yuan, J. Power Sources 175 (2008) 166.
[8] W.Z. Li, C.H. Liang, W.J. Zhou, J.S. Qiu, Z.H. Zhou, G.Q. Sun, Q. Xin, J. Phys. Chem. B 107 (2003) 6292.
[9] D. Li, Y.N. Xia, Adv. Mater. 16 (2004) 1151.
[10] G.Y. Han, G.Q. Shi, J. Appl. Polym. Sci. 103 (2007) 1490.
[11] X.Y. Wang, C. Drew, S.H. Lee, K.J. Senecal, J. Kumar, L.A. Sarnuelson, Nano Lett. 2 (2002) 1273.
[12] N. Bhattarai, Z.S. Li, D. Edmondson, M.Q. Zhang, Adv. Mater. 18 (2006) 1463.
[13] G.Y. Han, B. Guo, L.W. Zhang, B.S. Yang, Adv. Mater. 18 (2006) 1709.
[14] C. Kim, K.S. Yang, M. Kojima, K. Yoshida, Y.J. Kim, Y.A. Kim, M. Endo, Adv. Funct. Mater. 16 (2006) 2393.
[15] G.Y. Zhao, C.L. Xu, D.J. Guo, H. Li, H.L. Li, J. Power Sources 162 (2006) 492.